Rheological and thermal study of mixed cyclopentane + CO2 Hydrate slurries for refrigeration applications

Nada Chami, Yasmine Salehy, Pascal Clain, Didier Dalmazzone, Anthony Delahaye, L. Fournaison

Rheological and thermal study of mixed cyclopentane + CO$_2$ Hydrate slurries for refrigeration applications

Nada CHAMI[a,b], Yasmine SALEHY[b], Pascal CLAIN[b,c], Didier DALMAZZONE[a], Anthony DELAHAYE*[b], Laurence FOURNAISON[b]

[a] UCP/ENSTA Paris, Institut Polytechnique de Paris
91120, Palaiseau, France
[b] Université Paris-Saclay, INRAE, FRISE
92761, Antony, France
[c] Léonard de Vinci Pôle Universitaire, Research Center
92916 Paris la Défense, France
*Corresponding author: anthony.delahaye@inrae.fr

ABSTRACT

In order to reduce the amount of primary refrigerant, one solution could be the use of phase change material (PCM) slurries, such as gas hydrate slurries, in secondary loops. Previous studies have shown that cyclopentane (CP) acts as a thermodynamic promoter to form hydrates and to modify the equilibrium conditions toward lower pressure and higher temperature of CO$_2$ hydrates (having one of the higher melting enthalpy: 374 kJ.kg^{-1}). The present work is dedicated to the rheological and thermal study of simple CP hydrate and mixed CP + CO$_2$ hydrate slurries in a temperature-pressure controlled flow loop. For various concentrations of CP in oil-in-water emulsions (3-15wt%), the results showed that the viscosity of these slurries increases with a decreasing shear rate, exhibiting mostly a shear-thinning behaviour. Based on the heating tube method, the thermal characteristics of CP and CP + CO$_2$ hydrate slurries showed their ability to enhance heat transfer coefficients. The application of this secondary fluid can be refrigeration and air conditioning, depending on the temperature set by the operating conditions (pressure and CP composition).

Keywords: Secondary Loop Refrigeration, Slurry, Hydrates, Cyclopentane, Carbon dioxide

1. INTRODUCTION

In order to reduce the carbon footprint of refrigeration and air conditioning (RAC) systems, which account for 8-10% of global greenhouse gas emissions (IIF-IIR 2019), several approaches can be considered, such as secondary loop refrigeration. This method is known to significantly limit the amount of primary refrigerant (by a factor of about 10 (Wang et al. 2010)) by using environmentally friendly fluids in secondary loops (SL) which role is to transport thermal energy from the cold production machine (containing the confined primary refrigerant) to the places of use. SL refrigeration is often considered less efficient than direct expansion, due to an architecture requiring additional components (pumps, heat exchanger), but the use of two-phase secondary refrigerants in the form of phase change material (PCM) slurries can balance this loss of efficiency. Indeed, PCM slurries, consisting of a suspension of PCM particles, such as ice or hydrates, have much higher energy densities than single-phase secondary fluids. This is due to a latent heat of melting of PCMs (333 kJ.kg$_{water}^{-1}$ for ice, 500 kJ.kg$_{water}^{-1}$ for CO$_2$ hydrate (Marinhas et al. 2006)) much higher than the sensible heat of liquid single-phase secondary fluids. Thus, slurries can carry more energy for the same flow rate and are also more thermally stable, which improves machine efficiency. However, it is important to offer PCMs that are suitable for the temperature ranges of applications: ice, for example, is

compatible with application temperatures near 0 °C, but less suitable for higher temperature levels (air conditioning). CO_2 hydrates have adaptable temperature ranges, but require a pressure greater than 1 MPa. Gas hydrates are non-stoichiometric crystalline structures, made of water molecules like ice, but forming cages in which light gas molecules are enclosed. They are stable in conditions of low temperature and high pressure (Sloan 2003).

Considering the impact of PCM formation conditions on the efficiency of slurry-based SL refrigeration, several studies have been devoted to the use of thermodynamic promoters capable of adapting hydrate temperature and pressure conditions, such as tetrahydrofuran (THF) (Kang et al. 2001), tetrabutylammonium bromide (TBAB) (Lin 2007), tetra-n-butylphosphonium bromide (TBPB) (Mayoufi et al. 2012) and cyclopentane C5H10 (CP) (Zhang et al. 2009). These additives combine with gases to form mixed hydrates at lower pressures and higher temperatures than simple CO_2 hydrates and are themselves capable of forming simple hydrates at atmospheric pressure and low temperatures (Nakajima et al. 2008).

The present work investigates the use of CP as hydrate promoter in combination with CO_2. Several studies have been performed on thermodynamic conditions of simple CP hydrates and mixed CP+ CO_2 hydrates (Zhang et al. 2017; Lee et al. 2019; Chami et al. 2021). CP hydrates are stable at atmospheric pressure and in a temperature range from 279 to 285 K, which is well suited for air-conditioning applications. However, the latent heat of CP hydrate is 252 kJ.kg$_{water}^{-1}$ water, which is half the value of CO_2 hydrate and thus its storage capacity. Combining CP and CO_2 to form hydrate provides CP+CO_2 hydrates with higher latent heat, i.e. 462 kJ.kg$_{water}^{-1}$, close to the value of CO_2 hydrates, but at higher pressure between 0.01 to 0.45 MPa in the same temperature range from 279 to 285 K. Consequently, CP+CO_2 hydrates and to a lesser extent CP hydrates can be considered as good PCM material for cold storage. Nevertheless, in order to be implemented as PCM slurries in secondary loops, these hydrate slurries must present good flowability in the pipes. Therefore, a rheological characterization of simple CP and mixed CP + CO_2 hydrate slurry is necessary. In addition, for a thermal application such as secondary loop refrigeration, it is essential to characterize the ability of CP and CP+ CO_2 hydrate slurries to exchange heat.

In this work, a rheological characterisation of CP hydrate slurries and CP+ CO_2 hydrate slurries formed from direct O/W (Oil in Water) emulsions in a capillary viscometer is presented. This approach is original given that previous rheological studies on CP hydrate slurries were performed with rotational rheometer and very often using inverse W/O (Water in Oil) emulsions (Ahuja et al. 2015; Majid et al. 2019), while there are no data on the rheology of CP+ CO_2 hydrate slurries, except for our own work. In addition, the heat transfer coefficient of the CP hydrate slurry is investigated for the first time, based on the heating tube method.

2. MATERIALS AND METHODS

The following section describes materials and experimental procedure used to form hydrate slurries and to study rheology and heat transfer coefficient in dynamic loop.

2.1. Materials and emulsion preparation

2.1.1. Materials

The fluids used in the experiments were: distilled and degassed water; cyclopentane (CP) purchased from Acros Organics (Molar purity: 0.97); carbon dioxide purchased from Air Liquide (Molar purity: 0.99995). All materials were used without further purification. Properties of CP and CO_2 used are given in Table 1.

Table 1. Cyclopentane and carbon dioxide properties used in the present work

Name	Formula	Phase used	Solubility (cm3/100g of water)	Molar mass (g.mol^{-1})	Density (g.dm^{-3})	Latent heat (kJ.mol^{-1})
Carbon dioxide	CO_2	Gas	90.1 (at 293K)	44.01	1.87	15.33
Cyclopentane	C_5H_{10}	Liquid	Almost none	70.13	751	28.8

2.1.2. Emulsion preparation

Before performing the rheological and thermal characterization of CP and CP + CO_2 hydrate slurries, it is necessary to prepare a stock solution of the direct O/W emulsion of CP in water (also named CP/W emulsion). For this purpose, a mixture is prepared from water and a given amount of CP, corresponding to the desired CP fractions for the study: 3 wt%, 5 wt%, 7 wt%, 10 wt%, 12 wt%, and 15 wt%. These mixtures are then converted into an emulsion of O/W using a homogenizer (IKA T25 digital ULTRA TURRAX) operating at the speed of 18000 rpm for 15 min.

2.2. Experimental devices

Two devices were used for the present study:

- A loop under pressure for the rheological study of CP hydrate slurries and CP + CO_2 hydrate slurries

- A loop at atmospheric pressure for the thermal characterisation of CP hydrate slurries

2.2.1. Rheological loop

For the rheological characterisation, a loop located in a controlled cold room ensuring a homogeneous temperature of the circulating fluid inside the whole loop was used. This loop is composed of 344 mL stainless steel pipes with an 8 mm internal diameter and a 10 mm external diameter, and a glass cell to visualize hydrate slurries. It is also equipped with seven T-type thermocouples (±0.3 K), two pressure gauges from Sensit and Transintruments (0-5 MPa, ± 0.05 %), an electromagnetic flowmeter (IFM6080K-type Vatiflux, 0.5 %) (0-1800 L.h^{-1} ± 2.5%), and a pump (220-type, Maximum flow rate = 0.17 m^3.h^{-1}). The loop is equipped with a ABB 266 DSH differential pressure gauge (0-400 mbar ± 0.04 %) to measure pressure drops generated by the slurry. In order to form CO_2 hydrates under pressure, the loop is connected to a syringe pump (1000D ISCO) in order to apply calibrated injection (4 mL.min^{-1}) of CO_2. An illustration of the rheological loop is given in previous work (Clain et al. 2012).

2.2.2. Thermal loop

For the thermal characterisation, a loop connected to two coil heat exchangers was used to control the temperature of the circulating fluid. One of the heat exchangers can be used to form hydrate slurries, while the other can be used to melt hydrate slurries. This loop is also located in a controlled temperature cold room but only to ensure reproducible outdoor temperature conditions. Except for the presence of the heat exchangers, the configuration of the thermal loop is similar to that of the rheological loop, but with some differences. The thermal loop is composed of 368 mL stainless steel pipes with an 7.74 mm internal diameter and a 9.52 mm external diameter. It is also equipped with nine T-type thermocouples (±0.3 K), 6 PT100, three pressure gauges from Sensit and Transintruments (0-5 MPa, ± 0.05 %), a Rosemount 8732E Magnetic Flowmeter System (± 0.1% en précision), and a 220 type Axflow Micro Pump (Maximum flow rate = 0.2 m^3.h^{-1}). The loop is equipped with a ABB 265 DS differential pressure gauge (0-200 mbar ± 0.04 %) to measure pressure drops generated by the slurry. An illustration of the thermal loop is given in Figure 1.
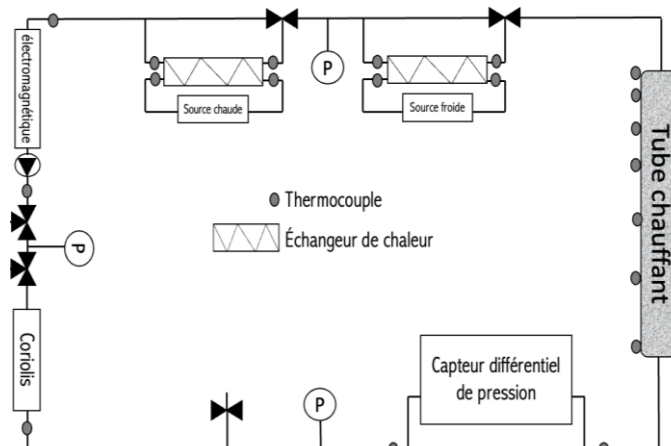
Figure 1: Scheme of the thermal loop

In order to measure the convective heat transfer coefficient (CHTC) of hydrate slurries, the heating tube method was used (right side of Figure 1). This method is described in the protocol section.

2.3. Experimental protocols

2.3.1. Hydrate slurry formation

After the preparation stage of the CP/W emulsion, the homogenized emulsion is immediately transferred to rheological or thermal loop.

In order to form CP hydrate slurries, the temperature is set at 272 K (lower than the equilibrium temperature of CP hydrates in pure water (Nakajima et al. 2008)), either in the rheological loop or in the thermal loop, with an initial flow rate of 120 L.h-1 and at atmospheric pressure. In the rheological loop, the temperature of the fluid is set using the controlled cold room, while in the thermal loop, the temperature of the fluid is set using one of the coil heat exchanger.

In the case of mixed CP + CO_2 hydrate slurry, the formation stage is performed in the rheological by cooling the CP-Water emulsion to a temperature of 280 K (lower than CP + CO_2 hydrate equilibrium temperature in pure water (Chami et al. 2021)) after applying a pressure around 1.5 MPa using calibrated CO_2 injection by syringe pump. The flow rate in the loop is identical to that of CP hydrate slurry, 120 L.h^{-1}.

During the temperature decrease, a sudden increase in pressure drop (measured by the differential pressure gauge) occurs when simple CP hydrates or mixed CP + CO_2 hydrates appear. This pressure drop increase is related to the increase in apparent viscosity of the fluid since hydrate slurries are more viscous than liquid phase. After thermodynamic and flow stabilization, the slurry with the desired hydrate fraction is formed, as illustrated in Figure 2. This hydrate fraction depends on the initial CP fraction in the CP/W emulsion.

Figure 2: Visualization of CP+ CO_2 hydrate slurries in the glass cell of the rheological loop

2.3.2. Rheological protocol

After hydrate slurry formation and stabilization of the system, the rheological analysis is achieved using a capillary viscometer, also known as Ostwald viscometer, described in previous work (Delahaye et al. 2011; Oignet et al. 2017a). It consists of circulating a fluid and determining its rheological parameters by relating the flow rate (or velocity) of the fluid to the pressure drop it generates in a straight pipe. The capillary

viscometer geometry is well suited to slurry flow loop. In addition, local heating due to friction is limited in a capillary viscometer, unlike rotary rheometers which have small gaps between their moving parts and can induce partial melting of hydrates.

The relationship between the flow rate and the pressure drop of the fluid in a capillary viscometer is based on a force balance, with several assumptions such as a laminar regime and the absence of wall slip (Steffe 1992). This force balance expresses the fact that a given quantity of fluid passing through a tube with a certain flow rate generates a pressure drop induced by the friction of the fluid on the wall. From this force balance, the following equation giving the flow rate as a function of shear stress and shear rate can be obtained:

$$\frac{Q}{\pi R^3} = \frac{1}{\tau_w{}^3} \int_0^{\tau_w} \tau^2 \dot{\gamma} \, d\tau \qquad \text{Eq. (1)}$$

where Q is the volume flow rate, R the pipe radius, $\dot{\gamma}$ the shear rate, τ the shear stress. τ_w is the shear stress at the wall, related to pressure drops ΔP in a pipe of length L and diameter D by the following equation:

$$\tau_w = \frac{D \, \Delta P}{4 \, L} \qquad \text{Eq. (2)}$$

After derivation of Eq. (2) with respect to τ_w, the Rabinowitsch-Mooney equation, giving an expression of $\dot{\gamma}_w$ the shear rate at the wall, is obtained:

$$\dot{\gamma}_w = \frac{3n + 1}{4n} \frac{8u}{D} \qquad \text{Eq. (3)}$$

where u is the flow velocity of the fluid, n the behaviour index defined as:

$$n = \frac{\partial (ln \, \tau_w)}{\partial \left(ln \frac{8u}{D} \right)} \qquad \text{Eq. (4)}$$

To implement the capillary viscometer method, various flow rates must be applied to cause pressure drops in order to correlate ΔP to u and thus τ_w to $\frac{8u}{D}$. Figure 3 shows an example of experimental data obtained when applying various flow rate plateaus resulting in various pressure drop plateaus.
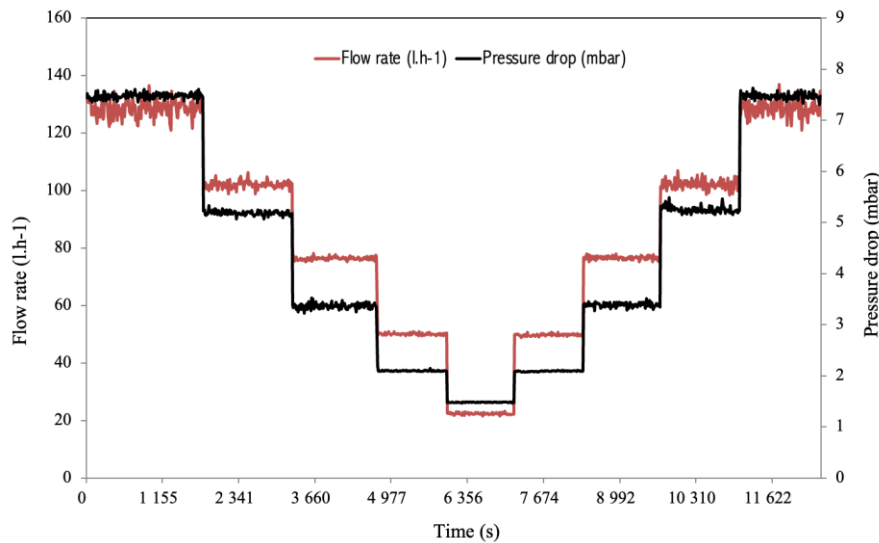

Figure 3: Example of experimental flow rate plateaus vs. pressure drop plateaus

The behavior index n is then deduced by linear regression, since it corresponds to the slope of the representative curve of the function $\ln(\tau_w) = f\left(\ln\left(\frac{8u}{D}\right)\right)$, according to Eq. (4). Depending on the value of n, the slurry can be considered as Newtonian ($n = 1$) or non-Newtonian, with a shear-thinning ($n < 1$) or shear-thickening ($n > 1$) type. Finally, knowing n, the shear rate $\dot{\gamma}_w$ is calculated based on Eq. (3). Various models can then be established to describe the rheological behavior of the slurry, such as the Herschel-Bulkley model:

$$\tau_w = \tau_0 + k\ \dot{\gamma}_w^n \qquad \text{Eq. (5)}$$

Where k and τ_0 are the consistency index and the yield stress, respectively, and can be obtained by linear regression since they corresponds to the slope and the y-intercept of the representative curve of the function $\tau_w = g(\dot{\gamma}^n)$. In addition, the apparent viscosity μ_app of the slurry can be defined as the ratio between the shear stress and the shear rate:

$$\mu_{app} = \frac{\tau_w}{\dot{\gamma}_w} \qquad \text{Eq. (6)}$$

2.3.3. Thermal protocol

The heating tube method, developped in previous work on ice slurries (Ionescu et al. 2007) and CO_2 hydrate slurries (Oignet et al. 2017b), was used in the present work to determine CHTC of hydrate slurries. This method is based on the use of a metallic tube (here in stainless steel of 620 mm length) subjected to an electric current to heat the tube by Joule effect. Thanks to the heating of the tube, a temperature difference is generated between the tube and hydrate slurries circulating inside. Knowing imposed heat flux and temperature differences involved, the heating tube method allows the characterization of CHTCs at different positions and thus the determination of the thermal settlement zone. It is then possible to characterize the values of the local CHTC independently of the position on the tube.

The heat flux $\dot{Q}$ is determined from the current and voltage applied to the tube wall via an electrical generator. The tube is heated by means of a Sorensen XFR power supply from MB electronic (6 V - 200 A - 2.8 kW) and is surrounded by Armaflex to be thermally isolated. The power supply is connected by two electrical cables to the ends of the tube, electrically isolated from the rest of the loop by two Swagelok PVC fittings resistant to a pressure of 3 MPa.

The tube temperature (Tp) is measured with seven thermocouples welded at different locations on the outer wall of the heating tube (Figure 4), while the slurry temperature (Tf) is measured with two PT100s in the circulating fluid (at the inlet and outlet of the heating tube). The slurry temperature along the tube is then estimated by applying a linear temperature profile of the fluid between the inlet and outlet of the tube.
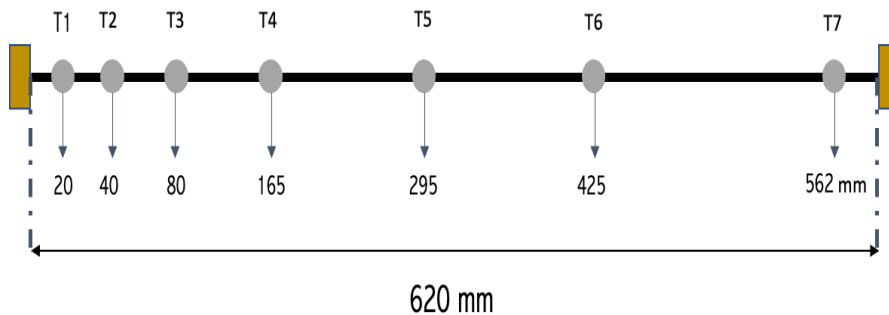

Figure 4: Scheme of the position of the thermocouples on the heating tube

The local exchange coefficients are then calculated for each position along the sensor by the following equation:

$$h_{loc}(x) = \frac{\dot{Q}(L)}{2\pi r L(T_p(x) - T_F(x) - \Delta T_p)}$$

Eq. (7)

where L corresponds to the length of the tube and ΔT_p to the difference between the temperature measured by the thermocouples at the external surface of the tube and the temperature at the internal surface of the tube (fluid-wall interface), defined as:

$$\Delta T_p = \left[\frac{\dot{Q}(L)}{4\pi\lambda_{tube}L}\right]\left[\frac{\xi(1 - ln\xi) - 1}{1 - \xi}\right]$$

Eq. (8)

where ξ represents the squared ratio between the outside and inside diameters of the tube.

3. RESULTS AND DISCUSSION

The following section describes the results and discussion related to the rheological and thermal study of hydrate slurries in dynamic loop.

3.1. Rheological properties of CP hydrate slurries and CP+ CO_2 hydrate slurries

As described in the materials and methods section, the rheological behavior is characterized by several criteria as the behavior index n. Figure 5 represents the evolution of the behavior index n of CP hydrate slurries and CP + CO_2 hydrate slurries as a function of CP fraction. The behavior index n of both slurries decreases with the increase of the CP fraction, which is a classical behaviour for slurries. Moreover, for CP fraction higher than 4 wt%, n becomes less than 1, which means that both hydrate slurries exhibit non-Newtonian behavior. Figure 5 also shows that n is greater than 1 for CP fraction less than 4 wt%, which is unusual rheo-thickening behaviour (maybe due to agglomeration or inertial effect).
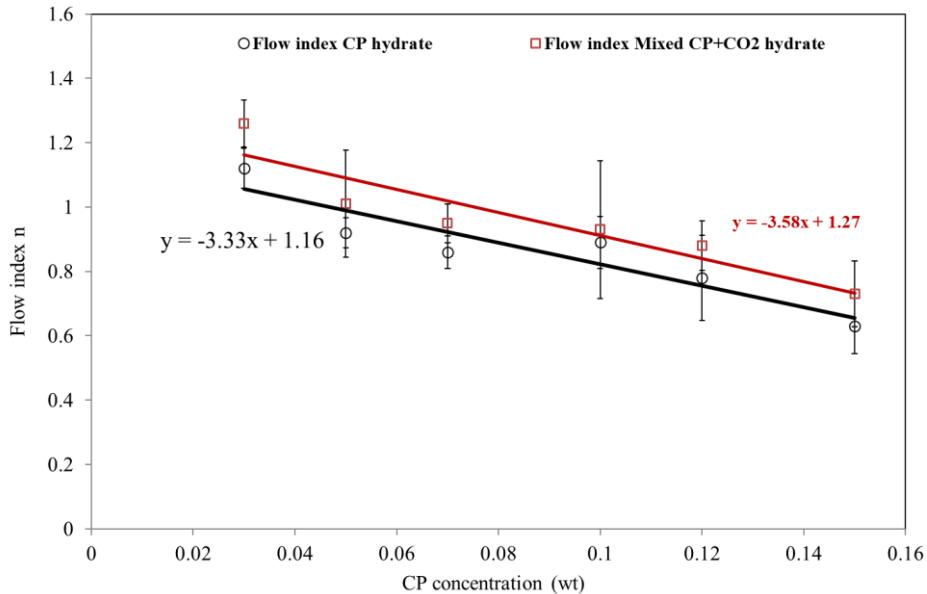

Figure 5: Behavior index n as a function of CP fraction for CP hydrate slurry and CP + CO_2 hydrate slurry

Based on Figure 5, the behavior index n was modelled as a function of CP fraction by Eq. (9) for CP hydrate slurry and by Eq. (10) for mixed CP + CO_2 hydrate slurry:

$$n = -3.33\, x_{CP} + 1.16 \qquad\qquad \text{Eq. (9)}$$

$$n = -3.58\, x_{CP} + 1.27 \qquad\qquad \text{Eq. (10)}$$

Knowing *n*, the consistency index *k* can be determined from linear regression based on Eq. (5), while the yield stress τ_0 is found to be equal to zero. The consistency index *k* can then be modelled as a function of CP fraction by Eq. (11) for CP hydrate slurry and by Eq. (12) for mixed CP + CO$_2$ hydrate slurry:

$$k = 0.0014\, e^{25.3 x_{CP}} \qquad\qquad \text{Eq. (11)}$$

$$k = 0.0004 e^{29.9 x_{CP}} \qquad\qquad \text{Eq. (12)}$$

The data of apparent viscosity can then be represented as a function of CP fraction. First, the experimental apparent viscosity μ_{app} are deduced from Eq. (6) and the experimental values of representing τ_w and $\dot{\gamma}$. Then the Herschel-Bulkley model (reduced to a power law) is determined based on the correlations of *n* and *k* from Eq. (9) to (12):
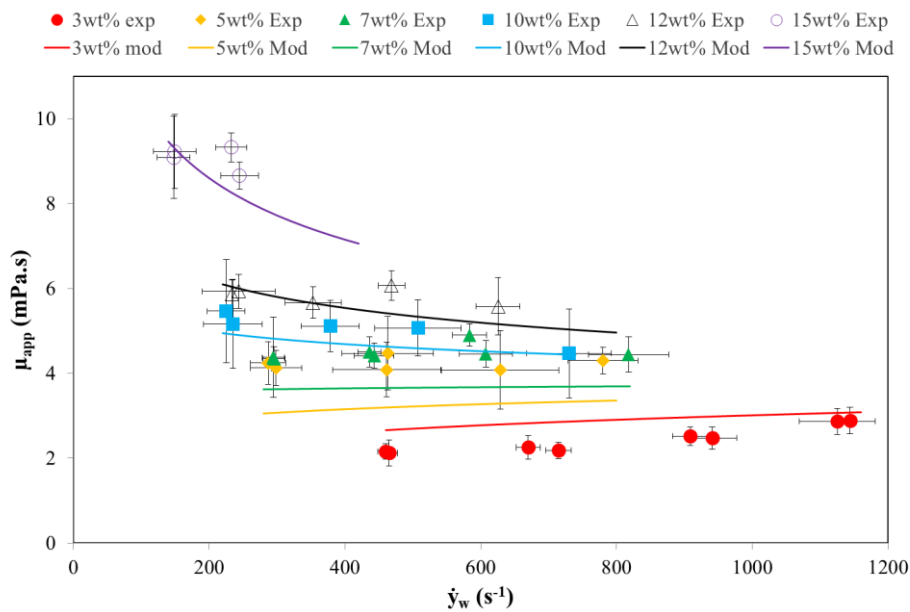
$$\tau_w = (0.0014 e^{25.3 x_{CP}}).\dot{\gamma}_w^{-3.33 x_{CP}+1.16} \qquad\qquad \text{Eq. (13)}$$

$$\tau_w = (0.0004 e^{29.9 x_{CP}}).\dot{\gamma}_w^{-3.58 x_{CP}+1.27} \qquad\qquad \text{Eq. (14)}$$

Eq. (13) and (14) are then combined to Eq. (6) to model the apparent viscosity as a function of CP fraction. Finally, experimental and modelled apparent viscosities are compared in Figure 6 and 7.
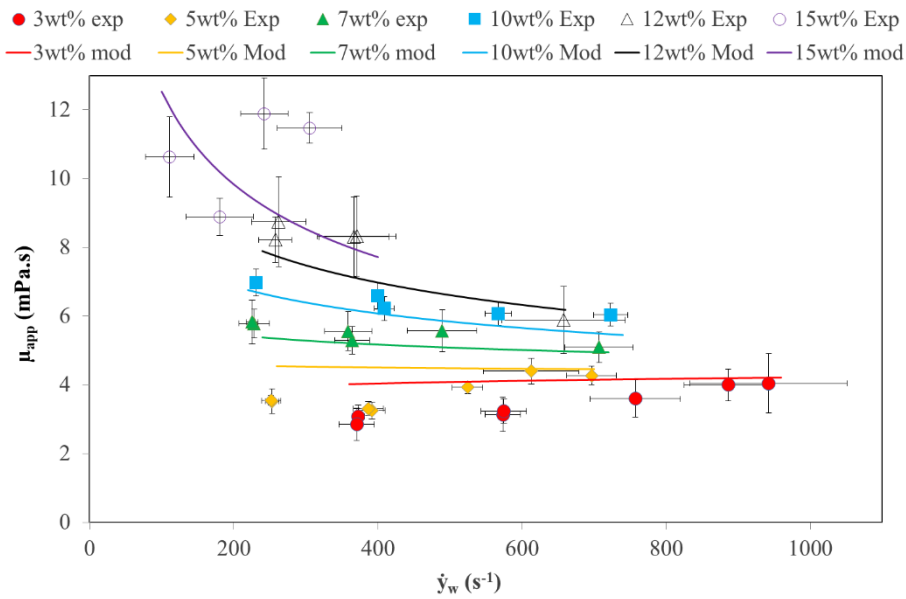
Figure 6: Apparent viscosity of CP hydrate slurry for CP fraction between 3 and 15wt %

Figure 7: Apparent viscosity of mixed CP + CO$_2$ hydrate slurry for CP fraction between 3 and 15wt%

As expected, it can be clearly seen that the apparent viscosity increases with the increasing amount of CP, and therefore of hydrate fraction, and the viscosity decreases when the applied shear rate increases for CP fractions above 7 wt% in cyclopentane, since the behavior index n is lower than 1. In addition, for CP fraction at 3 and 5 wt%, the viscosity does not show any dependence of the shear rate, since the behavior index is close to 1.

It is noticed that the data predicted by the model are generally in good agreement with those determined experimentally, with a slight difference that can be explained by an overestimation of the correlation of the consistency index k.

Table 2. Comparison of viscosities of CP hydrate slurry

Reference	Water cut (%)	Shear rate(s-1)	Viscosity (Pa. s)
Chen et al. (2021)	20	300	0.017±0.002
Liu et al.	20	300	0.014
This work (CP hydrate	85 88 90 93 95 97	300	0.011±0.0005 0.008±0.0015 0.007±0.0010 0.006±0.0006 0.004±0.0002 0.003±0.0005

In order to compare the present data to literature, Table 2 shows viscosity results from (Chen et al. 2021; Liu et al. 2021)Chen et al. and Liu et al. with the present results on CP hydrate slurries. Since all the experiments were performed with direct O/W (oil in water) emulsions in a capillary viscometer, unlike previous studies on CP hydrate slurry performed with inverse W/O (water in oil) emulsions in rotative rheometer, the comparison of viscosity values at the same shear rate should be considered with caution. Yet, Table 2 shows that the viscosity values found for hydrates formed from direct W/O emulsion and for

hydrate slurries formed from inverse O/W emulsion are close to each other and are of similar order. In particular, results at 20 % water cut in W/O emulsions are relatively close but higher to the present values at 85 % water cut in O/W emulsions, which is equivalent to 15 % CP cut. The difficulty is then to consider the appropriate rate of hydrate formation in order to convert the water threshold and CP threshold into a hydrate fraction, as it is likely that the conversion is not complete and that differences also exist between O/W or W/O emulsions (kinetic and surface limitation).

3.2.   Thermal properties of CP hydrate slurries and CP + CO$_2$ hydrate slurries

For the determination of convective heat transfer coefficients (CHTC) of CP hydrate slurries, the procedure was first verified on a water flow with CHTC values ranging from 600 to 2300 W.m^{-2}.K^{-1} depending on the Reynolds number, in good agreement with literature data (correlation of Hausen and correlation of correlation Schlünder). Then, measurement on CP hydrate slurries were perfomed with four different concentrations of CP: 3 wt%, 5 wt%, 7 wt%, and 10 wt%. In addition, the temperature of the thermostatic chamber is regulated at 10 °C and the temperature of the bath for cooling the CP/W emulsion is set at 0 °C. All tests are started by applying a heat flow in the heating tube with a power of 160 W. This power is chosen after several preliminary tests in order to limit the melting of hydrates (maximum power) while guaranteeing power independent data (minimum power related to the validity of the heating tube method).

Figure 8 shows the CHTC evolution of CP hydrate slurry formed from 7 wt% CP fraction as a function of axial position on the tube and for various Reynolds. The curves are characterized by a trend very similar to that of water, namely a slight increase and then decrease in the local heat exchange coefficient followed by a stabilization at the tube exit. This evolution along the tube has already been observed in other works using the heating tube method (Ionescu et al. 2007) and reflects the thermal settlement to be taken into account for the determination of the local CHTC. The CHTC varies between 900 and 2900 W.m^{-2}.K^{-1}. These values are higher than those of water, which confirms the interest of CP hydrate slurries for heat transfer.
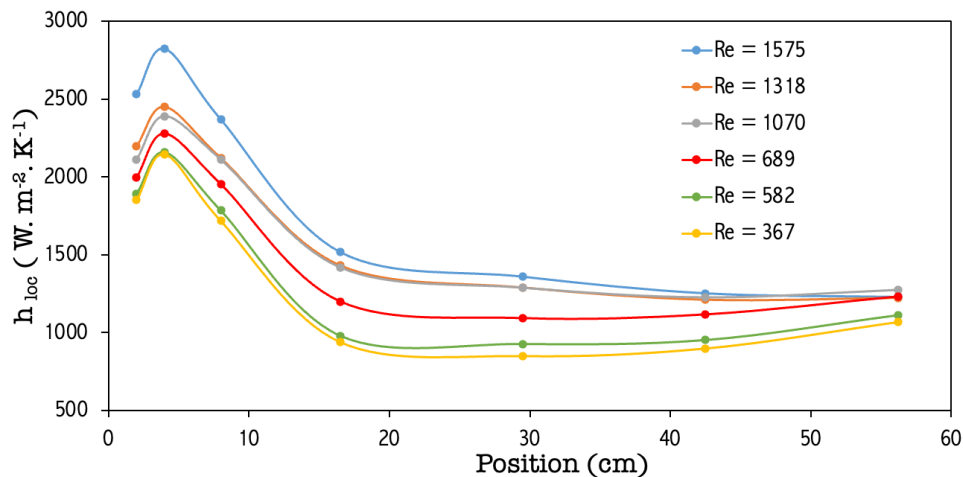

Figure 8: Apparent viscosity of mixed CP + CO$_2$ hydrate slurry for CP fraction between 3 and 15wt%

4.   CONCLUSIONS

A rheological and a thermal study of CP and mixed CP + CO$_2$ hydrate slurry in loop was carried out to understand the potential of this fluid for transportation application in secondary loop refrigeration. The following conclusions were drawn:

•   CP hydrate and mixed CP + CO$_2$ hydrate slurries exhibit mostly a shear-thinning behavior. This behavior becomes more evident with increasing CP concentration, significantly above 7 wt%.

- Semi-empirical models proposed to describe the effect of CP fraction on the rheological behavior of slurries are in good agreement with experimental data

- The apparent viscosity of CP and mixed CP + CO_2 hydrate slurry can be suitable for secondary loop application

- CHTC of CP hydrate slurries are higher than those of water and show the interest of CP hydrate slurries for heat transfer in secondary loop

In a further work, a coupled mass and thermal balance study could give indications on hydrate formation rates and thus allow to correlate the rheological and thermal data as a function of the actual hydrate fraction and not only as a function of the CP fraction. Given its enthalpy value and temperature controllability as a function of CO2 pressure and CP composition, this secondary fluid could be suitable for refrigeration and air-conditioning applications.

REFERENCES

Ahuja, A., Zylyftari, G., Morris, J. F. (2015). Yield stress measurements of cyclopentane hydrate slurry. Journal of Non-Newtonian Fluid Mechanics, 220, 116-125.

Chami, N., Bendjenni, S., Clain, P., Osswald, V., Delahaye, A., Fournaison, L., Dalmazzone, D. (2021). Thermodynamic characterization of mixed gas hydrates in the presence of cyclopentane as guest molecule for an application in secondary refrigeration. Chemical Engineering Science, 244, 116790.

Chen, Y., Shi, B., Fu, S., Li, Q., Yao, H., Liu, Y., Lv, X., Wang, J., Liao, Q., Duan, X., Gong, J. (2021). Kinetic and rheological investigation of cyclopentane hydrate formation in waxy water-in-oil emulsions. Fuel, 287, 119568.

Clain, P., Delahaye, A., Fournaison, L., Mayoufi, N., Dalmazzone, D., Fürst, W. (2012). Rheological properties of tetra-n-butylphosphonium bromide hydrate slurry flow. Chemical Engineering Journal, 193-194, 112-122.

Delahaye, A., Fournaison, L., Jerbi, S., Mayoufi, N. (2011). Rheological Properties of CO2 Hydrate Slurry Flow in the Presence of Additives. Industrial & Engineering Chemistry Research, 50(13), 8344-8353.

IIF-IIR (2019). Le rôle du froid dans l'économie mondiale. 38ème note d'information sur les technologies du froid, Institut international du froid - International Institute of Refrigeration.

Ionescu, C., Haberschill, P., Kiss, I., Lallemand, A. (2007). Local and global heat transfer coefficients of a stabilised ice slurry in laminar and transitional flows. International Journal of Refrigeration-Revue Internationale Du Froid, 30(6), 970-977.

Kang, S.-P., Lee, H., Ryu, B.-J. (2001). Enthalpies of dissociation of clathrate hydrates of carbon dioxide, nitrogen, (carbon dioxide + nitrogen), and (carbon dioxide + nitrogen + tetrahydrofuran). The Journal of Chemical Thermodynamics, 33(5), 513-521.

Lee, J., Kim, K.-S., Seo, Y. (2019). Thermodynamic, structural, and kinetic studies of cyclopentane + CO2 hydrates: Applications for desalination and CO2 capture. Chemical Engineering Journal, 375, 121974.

Lin, W. (2007). Effect of TBAB on thermal properties of CO2 hydrate. Antony, Cemagref.

Liu, Y., Lv, X., Shi, B., Zhou, S., Lei, Y., Yu, P., Chen, Y., Song, S., Ma, Q., Gong, J., Yan, K. (2021). Rheological study of low wax content hydrate slurries considering phase interactions. Journal of Natural Gas Science and Engineering, 94, 104106.

Majid, A. A. A., Tanner, B., Koh, C. A. (2019). Cyclopentane hydrate slurry viscosity measurements coupled with visualisation. Molecular Physics, 117(23-24), 3860-3870.

Marinhas, S., Delahaye, A., Fournaison, L., Dalmazzone, D., Fürst, W., Petitet, J.-P. (2006). Modelling of the available latent heat of a CO2 hydrate slurry in an experimental loop applied to secondary refrigeration. Chemical Engineering and Processing, 45(3), 184-192.

Mayoufi, N., Dalmazzone, D., Fürst, W., Elghoul, L., Seguatni, A., Delahaye, A., Fournaison, L. (2012). Phase behaviour of tri-n-butylmethylammonium chloride hydrates in the presence of carbon dioxide. Journal of Thermal Analysis and Calorimetry, 109(1), 481-486.

Nakajima, M., Ohmura, R., Mori, Y. H. (2008). Clathrate Hydrate Formation from Cyclopentane-in-Water Emulsions. Industrial & Engineering Chemistry Research, 47(22), 8933-8939.

Oignet, J., Delahaye, A., Torré, J.-P., Dicharry, C., Hoang, H. M., Clain, P., Osswald, V., Youssef, Z., Fournaison, L. (2017a). Rheological study of CO2 hydrate slurry in the presence of Sodium Dodecyl Sulfate in a secondary refrigeration loop. Chemical Engineering Science, 158, 294-303.

Oignet, J., Hoang, H.-M., Osswald, V., Delahaye, A., Fournaison, L., Haberschill, P. (2017b). Experimental study of convective heat transfer coefficients of CO2 hydrate slurries in a secondary refrigeration loop. Applied Thermal Engineering, 118, 630-637.

Sloan, E. D. (2003). Fundamental principles and applications of natural gas hydrates. Nature, 426(6964), 353-363.

Steffe, J. F. (1992). Rheological methods in food process engineering. East Lansing, MI, USA, Freeman Press.

Wang, K., Eisele, M., Hwang, Y., Radermacher, R. (2010). Review of secondary loop refrigeration systems. International Journal of Refrigeration, 33(2), 212-234.

Zhang, J. S., Lee, J. W. (2009). Equilibrium of Hydrogen + Cyclopentane and Carbon Dioxide + Cyclopentane Binary Hydrates. Journal of Chemical & Engineering Data, 54(2), 659-661.

Zhang, Y., Sheng, S.-M., Shen, X.-D., Zhou, X.-B., Wu, W.-Z., Wu, X.-P., Liang, D.-Q. (2017). Phase Equilibrium of Cyclopentane + Carbon Dioxide Binary Hydrates in Aqueous Sodium Chloride Solutions. Journal of Chemical & Engineering Data, 62(8), 2461-2465.